Journal of Magnetism and Magnetic Materials 322 (2010) 173–177

Contents lists available at ScienceDirect

Journal of Magnetism and Magnetic Materials

journal homepage: www.elsevier.com/locate/jmmm

Heat treatment effects on microstructure and magnetic properties of Mn–Zn ferrite powders

Ping Hu [a], Hai-bo Yang [b], De-an Pan [a], Hua Wang [a], Jian-jun Tian [a], Shen-gen Zhang [a,*], Xin-feng Wang [c], Alex A. Volinsky [d]

[a] School of Materials Science and Engineering, University of Science and Technology Beijing, Beijing 100083, PR China
[b] School of Mechanical Engineering, University of Science and Technology Beijing, Beijing 100083, PR China
[c] Beijing Electronic Science Vocational College, Beijing 100026, PR China
[d] Department of Mechanical Engineering, University of South Florida, Tampa, FL 33620, USA

ARTICLE INFO

Article history:
Received 15 July 2009
Received in revised form
21 August 2009
Available online 6 September 2009

Keywords:
Mn–Zn ferrite
Heat treatment
Microstructure
Magnetic property

ABSTRACT

Mn–Zn ferrite powders ($Mn_{0.5}Zn_{0.5}Fe_2O_4$) were prepared by the nitrate–citrate auto-combustion method and subsequently annealed in air or argon. The effects of heat treatment temperature on crystalline phases formation, microstructure and magnetic properties of Mn–Zn ferrite were investigated by X-ray diffraction, thermogravimetric and differential thermal analysis, scanning electron microscopy and vibrating sample magnetometer. Ferrites decomposed to Fe_2O_3 and Mn_2O_3 after annealing above 550 °C in air, and had poor magnetic properties. However, Fe_2O_3 and Mn_2O_3 were dissolved after ferrites annealing above 1100 °C. Moreover, the 1200 °C annealed sample showed pure ferrite phase, larger saturation magnetization (M_s=48.15 emu g^{-1}) and lower coercivity (H_c=51 Oe) compared with the auto-combusted ferrite powder (M_s=44.32 emu g^{-1}, H_c=70 Oe). The 600 °C air annealed sample had the largest saturation magnetization (M_s=56.37 emu g^{-1}) and the lowest coercivity (H_c=32 Oe) due to the presence of pure ferrite spinel phase, its microstructure and crystalline size.

1. Introduction

Mn–Zn ferrites are very important soft magnetic materials because of their high initial magnetic permeability, saturation magnetization, electrical resistivity and low power losses [1,2]. These materials are extensively used as inductors, transformers, antenna rods, loading coils, deflection yokes, choke coils, recording heads, magnetic amplifiers, electromagnetic interference devices (EMI), power transformers and splitters [3,4]. Moreover, Mn–Zn ferrites are very important in biomedicine as magnetic carriers for bioseparation, enzymes and proteins immobilization [5–8].

Recently, with the development of high frequency, low power miniaturized electronic devices, special focus has been placed on preparation of high performance Mn–Zn ferrite powders. To prepare high electromagnetic performance Mn–Zn ferrites, various synthesizing methods have been reported recently, including co-precipitation, alcohol dehydration, hydrothermal synthesis, spray drying, and sol–gel methods [9–13]. However, these methods are economically unfeasible for large-scale production. Recently more attention has been paid to the citrate–nitrate precursor auto-combustion method, which allows producing ultra-fine powders with chemically homogeneous composition, uniform size and good reactivity [14,15]. The advantages of this method are processing simplicity, low energy loss, high production efficiency and high-purity products.

In the present work, Mn–Zn ferrite powders were prepared by the citrate–nitrate precursor auto-combustion method. Then the as-prepared powders were annealed at different temperatures ranging from 400 to 1200 °C for 1 h in air and argon. Structural and magnetic properties of annealed Mn–Zn ferrites were investigated.

2. Experiment

Mn–Zn ferrite powders ($Mn_{0.5}Zn_{0.5}Fe_2O_4$) were prepared by the citrate–nitrate precursor auto-combustion method using ferric nitrate ($Fe(NO_3)_3 \cdot 9H_2O$), zinc nitrate ($Zn_2(NO_3) \cdot 6H_2O$), manganese nitrate ($Mn_2(NO_3)$), citric acid ($C_6H_8O_7 \cdot H_2O$) and ammonia as raw materials. Equimolar metal nitrates and citric acid were dissolved in appropriate amounts of distilled water, and the solution pH value was adjusted to 5.5 with ammonia. The solution was heated to 60 °C and continuously stirred using

* Corresponding author. Tel./fax: +86 10 62333375.
E-mail address: zhangshengen@mater.ustb.edu.cn (S.-g. Zhang).

0304-8853/$ - see front matter © 2009 Elsevier B.V. All rights reserved.
doi:10.1016/j.jmmm.2009.09.002

magnetic agitation. After 4 h the solution became a homogeneous viscous sol–gel. Then the sol–gel was oven dried at 120 °C for 24 h to obtain a dried gel. A loose, brown and very fine Mn–Zn ferrite powder was produced after the dried gel had spontaneously combusted in air.

In order to investigate the influence of annealing temperature on structural and magnetic properties, as-prepared auto-combusted $Mn_{0.5}Zn_{0.5}Fe_2O_4$ powders were annealed at 400, 550, 600, 700, 800, 900, 1000, 1100, and 1200 °C respectively for 1 h in air.

X-ray diffraction (XRD) was used to determine the phases and crystalline size. XRD patterns were recorded on a Philips APD-10 diffractometer using Cu-K_α source. Thermogravimetric and differential thermal analysis (TG-DTA) (METTLER TOLEDO STAR^e system, Switzerland) of the auto-combusted ferrites was carried out with a heating rate of 10 °C/min in air. The morphology and size of particles were observed by scanning electron microscopy (SEM) (LEO 1450). LDJ 9600 (LDJ Electronics, Troy, MI, USA) vibrating sample magnetometer (VSM) was used to investigate the magnetic properties at room temperature.

3. Results and discussion

3.1. Products phase analysis

Fig. 1 shows XRD patterns of the auto-combusted powder and samples annealed at different temperatures ranging from 400 to 1200 °C for 1 h in air. The as-prepared auto-combusted powder has a pure spinel structure (JCPDS 74-2401), which indicates that one can obtain a pure Mn–Zn ferrite phase by the method of citrate–nitrate precursor auto-combustion. At low 400 °C annealing temperature, powders also have pure spinel structure. However, above 550 °C, the annealed powders contain some impurity XRD reflections, which are due to the Fe_2O_3 and Mn_2O_3 phases (JCPDS 33-0664 and 24-0508). Fe_2O_3 and Mn_2O_3 begin to dissolve at 1100 °C. Moreover, at 1200 °C, a well-crystallized pure Mn–Zn ferrite phase is formed.

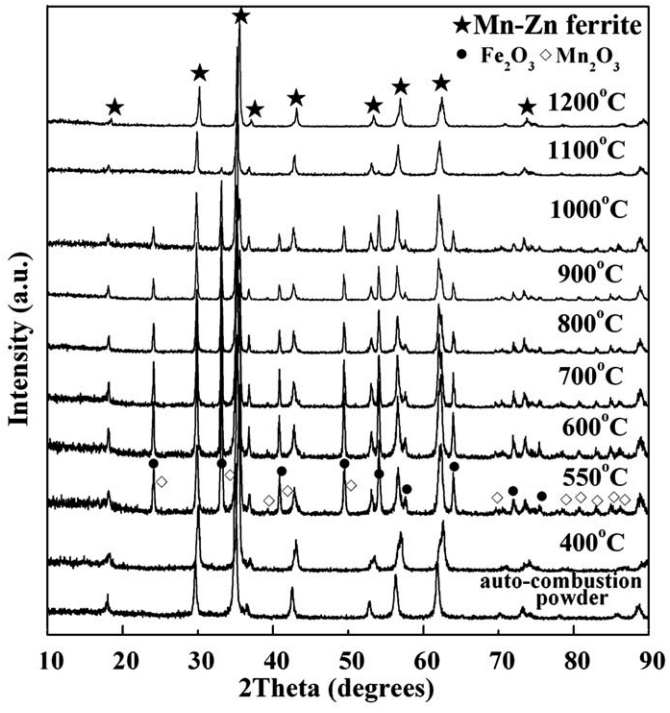

Fig. 1. XRD patterns of $Mn_{0.5}Zn_{0.5}Fe_2O_4$ powders annealed at different temperatures.

Fig. 2 shows the effect of the annealing temperature on the crystalline sizes of the annealed powders. The average crystalline sizes were determined using the Debye–Scherrer's formula [16]. The crystalline size of auto-combusted powder is about 23.6 nm. The crystallite sizes of annealed powders first increases from 24.8 to 39.8 nm with the annealing temperature increase from 400 to 1100 °C. Then it decreases to 32.9 nm at 1200 °C. The reason for the decrease will be explained later.

3.2. TG-DTA analysis of ferrite powders auto-combustion

In order to investigate the mechanism of the Mn–Zn ferrites auto-combustion, thermal analysis (TG-DTA) was carried out and the results are shown in Fig. 3. In the DTA curve, the 541.4 °C endothermic peak is relatively sharp and intense; however, the TG curve is quite flat. With annealing temperature increase, there is an intense 1043.01 °C exothermic peak in the DTA curve, and the TG curve exhibits continuous weight loss here.

Mn and Fe elements have varying valencies in Mn–Zn ferrites, therefore, oxidation and reduction reactions would probably occur in Mn–Zn ferrites. The reactions would depend on the oxygen partial pressure in the environment and the heat treatment

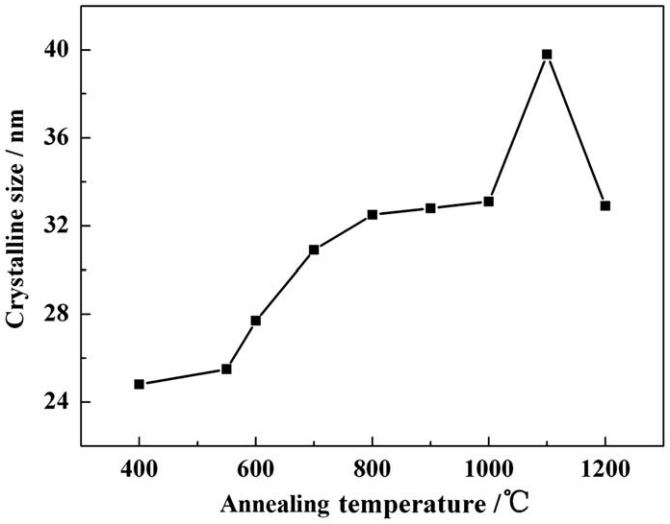

Fig. 2. Mn–Zn ferrite crystalline size dependence on the annealing temperature.

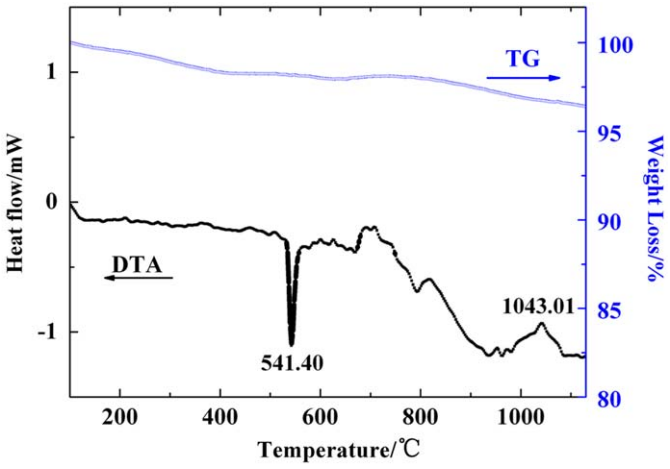

Fig. 3. TG-DTA curves of Mn–Zn ferrite powders.

temperature. Mn–Zn ferrites decomposition pressure is lower than the oxygen partial pressure in air, thus ferrites tend to oxidize at low annealing temperature in air. When the oxygen partial pressure is higher than the ferrite decomposition pressure, the decomposition reaction in ferrites occurs [17]:

$$MnFe_2O_4 + [O] \rightarrow Fe_2O_3 + Mn_2O_3 \quad (1)$$

Fe_2O_3 and Mn_2O_3 cannot be dissolved in the Mn–Zn ferrite with cubic spinel structure due to their body-centered cubic (BCC) structure. Therefore, Fe_2O_3 and Mn_2O_3 precipitate from the Mn–Zn ferrite phase as separate BCC phases. With annealing temperature increase, the inner oxygen pressure in the samples increases [18]. When the inner oxygen pressure in samples is higher than the environment oxygen partial pressure, Mn–Zn ferrites are formed again according to a combination reaction [17]:

$$Fe_2O_3 + Mn_2O_3 \rightarrow MnFe_2O_4 \rightarrow MnZn - Ferrite \quad (2)$$

TG-DTA results are in good agreement with the above mechanism and XRD patterns shown in Fig. 1. The endothermic peak at 541.4 °C in the DTA curve is due to the Mn–Zn ferrites decomposition reaction (1). Annealed powders have Fe_2O_3 and Mn_2O_3 impurities when the annealing temperature is higher than 550 °C. However, in our experiments, the annealed powders also have a single ferrite phase below 541.4 °C (400 °C annealing temperature), possibly due to very slow diffusion rate at lower temperatures. Reaction (2) happened at 1043.01 °C, and above this temperature, the Fe_2O_3 and Mn_2O_3 impurities disappeared. A well-crystallized single Mn–Zn ferrite phase was formed. This combination of ferrite phase and recrystallization causes the crystallite size decrease at 1200 °C annealing temperature (Fig. 2). Therefore, it is very important to control the environment oxygen partial pressure for producing pure Mn–Zn ferrites.

3.3. Experiment verification

Fig. 4 shows XRD patterns of powders when auto-combusted ferrite was annealed at 600 °C for 1 h in argon atmosphere. All of the detectable diffraction reflections are well indexed as pure cubic spinel ferrite phase and no diffraction of other impurities is observed in the patterns. Compared with the powder annealed at 600 °C for 1 h in air, the argon-annealed Mn–Zn ferrites do not decompose according to reaction (1) due to the lower oxygen partial pressure in protective argon atmosphere than in air. This also validates the above mechanism of auto-combusted Mn–Zn ferrite powders annealing at different temperatures.

Meanwhile, Fig. 5 shows XRD patterns of pure Mn–Zn ferrite phase annealed at different conditions. The sample annealed in argon at 600 °C has the sharpest and most intense XRD reflections compared with the other three diffraction patterns, indicating good crystallinity. On the other hand, the sample annealed in air at 1200 °C has sharper and more intense diffraction reflections than the sample annealed in air at 400 °C, which has approximate equal diffraction reflections intensity as the auto-combusted ferrite powder.

3.4. Products microstructure evolution with annealing temperature

Typical SEM micrographs of $Mn_{0.5}Zn_{0.5}Fe_2O_4$ ferrite microstructure annealed for 1 h in air at 600 and 1200 °C are shown in Fig. 6. It is clear that there is larger powder particles size with increased annealing temperature. As seen in Fig. 6(a), auto-combustion ferrite powders are uniform in both morphology and particle size, but are agglomerated to some extent due to interactions between magnetic nanoparticles. Fig. 6(b) shows microstructure with precipitation and open porosity, due to the Fe_2O_3 and Mn_2O_3 impurities at the 550 °C annealing temperature and above. As the annealing temperature is increased to 1200 °C (Fig. 6(c)), a clear homogenous crystalline structure is observed.

3.5. Magnetic properties

Magnetic properties were measured by the VSM at room temperature for the auto-combusted ferrite powder and samples annealed at 600 and 1200 °C in air, and at 600 °C in argon, as shown in Fig. 7, respectively. The magnetic properties data, crystalline size and phases of samples annealed at different temperature are listed in Table 1. It is clear that the auto-combusted ferrite powder and samples annealed at 1200 °C in air and 600 °C in argon have magnetic properties superior to the same composition ferrites prepared by other techniques [4,19]. On the

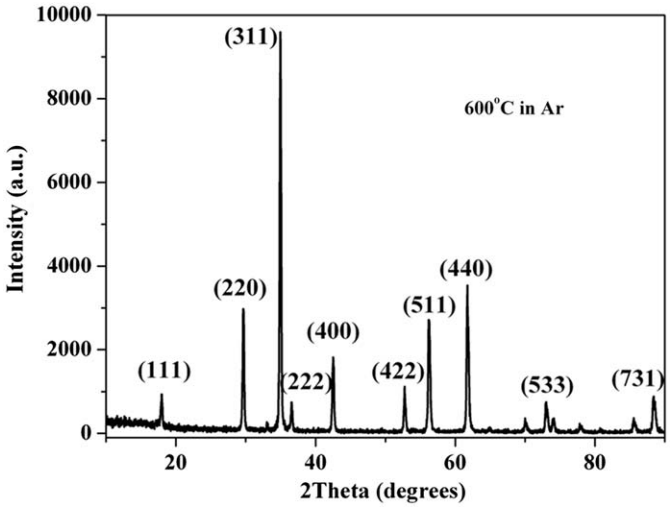

Fig. 4. XRD patterns of annealed powder at 600 °C in argon.

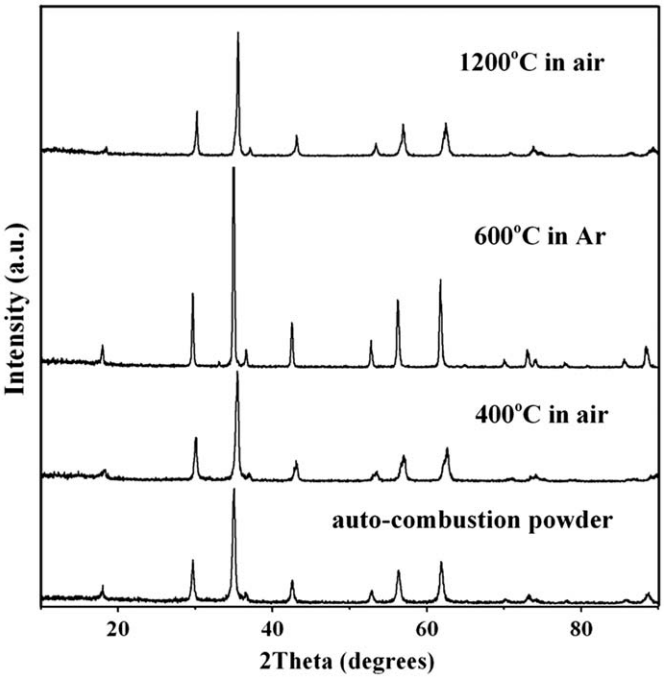

Fig. 5. XRD patterns of pure Mn–Zn ferrite phase annealed at different conditions.

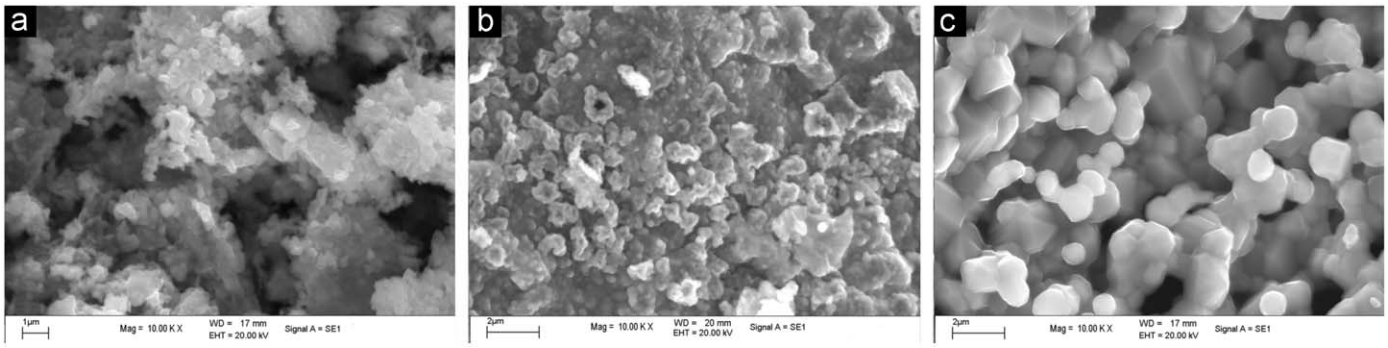

Fig. 6. SEM micrographs of powders annealed at different temperatures in air: (a) auto-combustion powder; (b) annealed at 600 °C and (c) at 1200 °C.

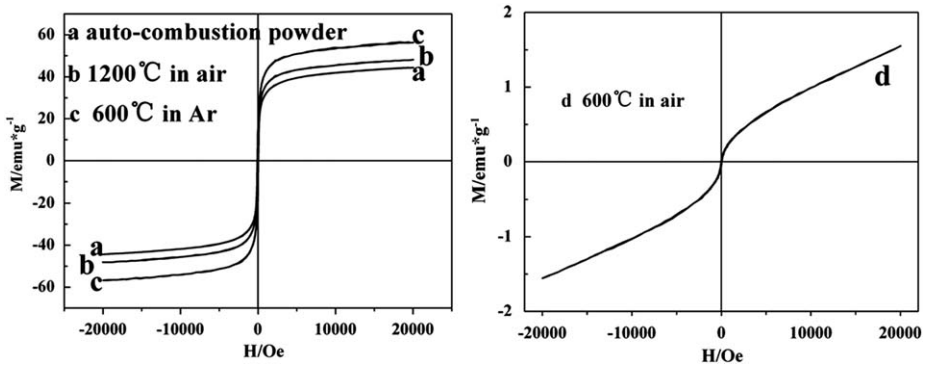

Fig. 7. Magnetic hysteresis loops of powders annealed at different temperatures.

Table 1
Magnetic properties, crystalline size and phases of powders annealed at different temperatures.

Samples	M_s (emu g^{-1})	M_r (emu g^{-1})	H_c (Oe)	Crystalline size (nm)	Phase
Auto combustion power	44.32	12.31	70	23.6	Mn–Zn ferrite
1200 °C in air	48.15	8.724	51	32.9	Mn–Zn ferrite
600 °C in air	56.37	13.72	32	45.1	Mn–Zn ferrite
600 °C in air	1.552	0.03489	29	27.7	Ferrite and impurities

contrary, the sample annealed at 600 °C in air has poor magnetic properties due to the appearance of non-magnetic Fe_2O_3 and Mn_2O_3 impurities.

Comparing the magnetic properties of the three pure ferrite phase samples, the sample annealed in argon at 600 °C has the largest saturation magnetization (M_s=56.37 emu g^{-1}) and the lowest coercivity (H_c=32 Oe). The sample annealed in air at 1200 °C has larger saturation magnetization (M_s=48.15 emu g^{-1}) and lower coercivity (H_c=51 Oe) than the auto-combusted ferrite powder. This can be attributed to an increase in crystallinity, microstructure and crystalline sizes of the formed ferrite phase as shown in Table 1 and Fig. 5. It is known that saturation magnetization gradually increases with the crystalline size and coercivity, which is defined by decreased domain walls displacement as the crystalline size increases in the multi-domain range [20].

4. Conclusions

Nanocrystalline $Mn_{0.5}Zn_{0.5}Fe_2O_4$ ferrite powders were prepared by the nitrate–citrate auto-combustion method. The crystalline size of auto-combusted ferrite powders is about 23.6 nm. The effects of heat treatment on the structural and magnetic properties of the auto-combusted ferrite samples were investigated. Ferrites decomposed to Fe_2O_3 and Mn_2O_3 after annealing at 550 °C in air, which have poor magnetic properties. With continuously increased annealing temperature, Fe_2O_3 and Mn_2O_3 impurities were dissolved when the annealing temperature rose above 1100 °C. The sample annealed at 1200 °C showed pure Mn–Zn ferrite phase, which had fine crystallinity, uniform particle sizes, and showed larger saturation magnetization (M_s=48.15 emu g^{-1}) and the lower coercivity (H_c=51 Oe) than the auto-combusted ferrite powder (M_s=44.32 emu g^{-1}, H_c=70 Oe). The sample annealed in argon at 600 °C had the largest saturation magnetization (M_s=56.37 emu g^{-1}) and the lowest coercivity (H_c=32 Oe). This could be attributed to an increase in phase formation, crystallinity, microstructure and crystalline sizes.

Acknowledgments

The authors gratefully acknowledge support provided by the National Natural Science Foundation of China (Nos. 50874010, 50802008), Key Projects in the National Science & Technology Pillar Program of China (No. 2009BAE74B00) and Program for New Century Excellent Talents in University (NCET). Alex A. Volinsky would like to acknowledge NSF support (CMMI-0600266).

References

[1] G. Ott, J. Wrba, R. Lucke, J. Magn. Magn. Mater. 535 (2003) 254–255.
[2] U. Ghazanfar, S.A. Siddiqi, G. Abbas, Mater. Sci. Eng. B 118 (2005) 84.
[3] S.H. Keluskar, R.B. Tangsali, G.K. Naik, J.S. Budkuley, J. Magn. Magn. Mater. 305 (2006) 296–303.
[4] M.M. Hessien, M.M. Rashad, K. El-Barawy, I.A. Ibrahim, J. Magn. Magn. Mater. 320 (2008) 1615–1621.
[5] R. Arulmurugan, B. Jeyadevan, G. Vaidyanathan, S. Sendhilnathan, J. Magn. Magn. Mater. 288 (2005) 470.
[6] P. Papazoglou, F. Eleftheriou, V.T. Zaspalis, J. Magn. Magn. Mater. 296 (2006) 25.
[7] C. Upadhyay, H.C. Verma, C. Rath, K.K. Sahu, S. Anand, R.P. Das, N.C. Mishra, J. Alloys Compd. 326 (2001) 94.
[8] A.C.F.M. Costa, E. Tortella, M.R. Morelli, R.H.G.A. Kiminami, J. Magn. Magn. Mater. 256 (2003) 174.
[9] I.Z. Rahman, T.T. Ahmed, J. Magn. Magn. Mater. 290–291 (2005) 1576–1579.
[10] P. Sainamthip, V.R.W. Amarakoon, J. Am. Ceram. Soc. 71 (2) (1988) C92–C95.
[11] S. Komarneni, E. Fregeau, E. Breval, R. Roy, J. Am. Ceram. Soc. 71 (1) (1988) C26–C28.
[12] X. Zhao, B. Zheng, H. Gu, C. Li, S.C. Zhang, P.D. Ownby, J. Mater. Res. 14 (7) (1999) 3073–3082.
[13] S. Yan, J. Geng, L. Yin, E. Zhou, J. Magn. Magn. Mater. 277 (2004) 84–89.
[14] A.R. Bueno, M.L. Gregori, M.C.S. N′obrega, Mater. Chem. Phys. 105 (2007) 229–233.
[15] A. Verma, R. Chatterjee, J. Magn. Magn. Mater. 306 (2006) 313–320.
[16] H.P. Klug, L.E. Alexander, X-ray Diffraction Procedures for Polycrystalline and Amorphous Materials, John Wiley and Sons, New York, 1997, p. 637.
[17] Z.G. Zhou, Ferrite Magnetic Materials, Science Press, Beijing, 1981 pp. 368–374.
[18] M. El Guendouzi, K. Sbai, P. Perriat, B. Gillot, Mater. Chem. Phys. 25 (1990) 429–436.
[19] Z.G. Zheng, X.C. Zhong, Y.H. Zhang, H.Y. Yu, D.C. Zeng, J. Alloys Compd. 466 (2008) 377–382.
[20] L. Zhao, H. Yang, L. Yu, Y. Cui, X. Zhao, B. Zou, S. Feng, J. Magn. Magn. Mater. 301 (2006) 445.